

Expression Patterns of a Novel *AtCHX* Gene Family Highlight Potential Roles in Osmotic Adjustment and K^+ Homeostasis in Pollen Development^{1[w]}

Heven Sze*, Senthilkumar Padmanaban, Françoise Cellier, David Honys, Ning-Hui Cheng, Kevin W. Bock, Genevieve Conéjéro, Xiyan Li, David Twell, John M. Ward, and Kendal D. Hirschi

Department of Cell Biology and Molecular Genetics, University of Maryland, College Park, Maryland 20742–5815 (H.S., S.P., K.W.B., X.L.); Biochimie et Physiologie Moléculaire des Plantes, Unité Mixte de Recherche 5004 Institute National de la Recherche Agronomique/Centre National de la Recherche Scientifique/AgroM/Université Montpellier II, 34060 Montpellier cedex, France (F.C., G.C.); Laboratory of Pollen Biology, Institute of Experimental Botany Academy of Sciences of the Czech Republic, 16502 Prague 6, Czech Republic (D.H.); Departments of Pediatrics and Human and Molecular Genetics, Children's Nutrition Research Center, Baylor College of Medicine, Houston, Texas 77030 (N.-H.C., K.D.H.); Department of Biology, University of Leicester, Leicester LE1 7RH, United Kingdom (D.T.); and Department of Plant Biology, University of Minnesota, St. Paul, Minnesota 55108 (J.M.W.)

A combined bioinformatic and experimental approach is being used to uncover the functions of a novel family of cation/ H^+ exchanger (*CHX*) genes in plants using *Arabidopsis* as a model. The predicted protein (85–95 kD) of 28 *AtCHX* genes after revision consists of an amino-terminal domain with 10 to 12 transmembrane spans (approximately 440 residues) and a hydrophilic domain of approximately 360 residues at the carboxyl end, which is proposed to have regulatory roles. The hydrophobic, but not the hydrophilic, domain of plant *CHX* is remarkably similar to monovalent cation/proton antiporter-2 (CPA2) proteins, especially yeast (*Saccharomyces cerevisiae*) KHA1 and *Synechocystis* NhaS4. Reports of characterized fungal and prokaryotic CPA2 indicate that they have various transport modes, including K^+/H^+ (KHA1), Na^+/H^+-K^+ (GerN) antiport, and ligand-gated ion channel (KefC). The expression pattern of *AtCHX* genes was determined by reverse transcription PCR, promoter-driven β -glucuronidase expression in transgenic plants, and Affymetrix ATH1 genome arrays. Results show that 18 genes are specifically or preferentially expressed in the male gametophyte, and six genes are highly expressed in sporophytic tissues. Microarray data revealed that several *AtCHX* genes were developmentally regulated during microgametogenesis. An exciting idea is that *CHX* proteins allow osmotic adjustment and K^+ homeostasis as mature pollen desiccates and then rehydrates at germination. The multiplicity of *CHX*-like genes is conserved in higher plants but is not found in animals. Only 17 genes, *OsCHX01* to *OsCHX17*, were identified in rice (*Oryza sativa*) subsp. *japonica*, suggesting diversification of *CHX* in *Arabidopsis*. These results reveal a novel *CHX* gene family in flowering plants with potential functions in pollen development, germination, and tube growth.

The ability to complete the plant life cycle depends not only on uptake of essential minerals, but also on the distribution and sorting of each ion to specific tissues, cell types, and organelles at all developmental stages. How plants achieve this under environments containing widely different levels of mineral nutrients is still poorly understood. This resilience can be attributed in part to a large number of transporters with

varying ion specificities and affinities, and signal transduction networks that modulate the activities of each transporter. In spite of the remarkable advances since the discovery of the essential nutrients by Hoagland (1944), until recently we had no idea about the total number or types of transporters required to complete the plant life cycle.

The completed *Arabidopsis* genome revealed more than 800 predicted transporters, of which most are secondary active transporters (>65%; *Arabidopsis* Genome Initiative, 2000). Most cotransporters depend on the proton electrochemical gradient generated by primary proton pumps and have been classified based on both phylogeny and function as transporters for cation, anion, and C- and N-containing compounds, including sugars, amino acids, drugs, and toxins (*Arabidopsis* Genome Initiative, 2000; Saier, 2000). Within the secondary active transporters, we had

¹ This work was supported in part by the National Science Foundation *Arabidopsis* 2010 Project (grant nos. IBN0209788 and IBN0200093 to H.S., 0209792 to J.M.W., and 020977 to K.H.) and by a Royal Society/NATO Fellowship and the Ministry of Education of the Czech Republic (grant no. 1K03018 to D.H.).

* Corresponding author; e-mail hsze@umd.edu; fax 301–314–9081.

^[w]The online version of this article contains Web-only data.

Article, publication date, and citation information can be found at www.plantphysiol.org/cgi/doi/10.1104/pp.104.046003.

found 44 genes predicting proteins that belonged to the monovalent cation proton antiporter (CPA) superfamily, according to the Transport Classification (TC) system of Saier (2000). Preliminary phylogenetic analyses separated this group of genes, named *NHX*, *CHX*, and *KEA*, into two families, CPA1 (TC 2.A.36) and CPA2 (TC 2.A.37; Maser et al., 2001).

The best examples of CPAs in plants are those that extrude excess Ca^{2+} or Na^+ from the cytosol either into vacuolar and endomembrane compartments or to the extracellular space. Eleven members of the CaCA family in Arabidopsis, named *CAX1* to *CAX11*, encode Ca^{2+} or divalent cation exchangers. These transporters, although related to CPA, form a separate clade in phylogenetic analyses (Maser et al., 2001). Of eight *NHX* family members in Arabidopsis CPA1, several have been functionally identified as Na^+/H^+ exchangers after cDNA expression in yeast (*Saccharomyces cerevisiae*) mutants. The best characterized include AtNHX1 (Gaxiola et al., 1999) that sequesters Na^+ into vacuoles and the plasma membrane (PM)-localized SOS1/AtNHX7 (Shi et al., 2002). Ectopic expression of *AtNHX1* causes dramatic salt tolerance in Arabidopsis (Apse et al., 1999). AtNHX1 is localized to plant vacuoles and is highly expressed in all organs. Its role as a Na^+/H^+ antiporter was demonstrated by Na^+ dissipation of a pH gradient (acid inside) in vacuoles from plants overexpressing AtNHX1. *SOS1* is primarily expressed in the xylem parenchyma (Shi et al., 2002), and both transcript level and Na^+/H^+ antiport activity in PM vesicles are enhanced after plant exposure to high salt (Shi et al., 2000; Qiu et al., 2002). Overexpression of *SOS1* reduces Na content and improves salt tolerance of transgenic Arabidopsis (Shi et al., 2003).

We embarked on a project to determine the functions of a novel *CHX* family in plants by a combination of bioinformatic and experimental approaches. As Na^+ is not an essential nutrient for glycophytes, it was surprising to find more than 20 Arabidopsis genes other than *NHX*s classified as Na^+/H^+ transporters in the databases. Here, we conducted phylogenetic analyses of 28 Arabidopsis and 17 rice (*Oryza sativa*) *CHX* proteins. We show that all predicted *CHX* proteins are similar in size, with approximately 800 residues that consist of a hydrophobic transport domain at the amino terminus and a putative regulatory domain at the carboxyl terminus. However, CPA2-like proteins have not been reported in the fly, worm, or human genomes, suggesting that multiple *CHX* proteins perform functions characteristic of higher plants. The similarity of plant *CHX* proteins to characterized fungal and bacterial CPA2 suggests that plant *CHX* proteins transport K^+ , Na^+ , and H^+ in various catalytic modes. We show for the first time that expression of 18 *AtCHX* genes is, surprisingly, either pollen specific or pollen enhanced, and only 6 are expressed highly in vegetative tissues. These findings highlight for the first time the potential importance of multiple *CHX* genes in the develop-

ment, survival, and function of the male gametophyte.

RESULTS

CHX Genes Encode a Large Family of CPA2-Like Proteins with Approximately 800 Residues in Arabidopsis

As a first step to define the functions of the large monovalent CPA2 family, we revised the predicted *CHX* protein sequence from Arabidopsis using the following strategy. cDNA sequences were used whenever possible to predict protein sequence. In the absence of cDNA sequence, the genomic sequences were translated and the intron/exon borders were revised manually. Multiple protein sequence alignments were produced for each clade and used to identify possible errors in splice-site prediction. Conserved splice sites, often found in the products of gene duplication, were used to predict intron/exon splicing. As a result, revised predicted sequences were produced for nearly one-third of the AtCHX proteins. Revisions included altered translational start sites and changes to predicted splice sites. In one case, AtCHX06, initially part of AtCHX05 (2,658 residues), was later predicted to encode a protein of 1,536 residues, and then split into two *CHX* genes in tandem, *CHX06a* (At1g08140) and *CHX06b* (At1g08135). After revision, we found that predicted *CHX* proteins range from 770 to 867 residues, with molecular masses of 85 to 95 kD (Table I; Supplemental Fig. 1, available at www.plantphysiol.org). All *CHX* isoforms are predicted to consist of a hydrophobic amino-terminal domain with 10 to 12 transmembrane (TM) α -helices (410–470 residues) and a carboxyl hydrophilic domain of 328 to 420 residues. Phylogenetic analyses showed this family could be separated into several subclades (Fig. 1A). BLAST or conserved-domain analyses consistently classified the *CHX* proteins as having a Na^+/H^+ exchanger domain characteristic of proteins in the CPA1 family.

Phylogenetic analyses showed that the only eukaryotic proteins close to plant *CHX* are from fungi (TransportDB; <http://66.93.129.133/transporter/wb/index2.html>). The best-characterized fungal CPA2 is the yeast KHA1, a putative K^+/H^+ exchanger (Ramirez et al., 1998). We compared various AtCHX proteins with monovalent cation/ H^+ antiporters from the CPA superfamily, including rat NHE1 (Orlowski et al., 1992), yeast KHA1 (Ramirez et al., 1998), Arabidopsis NHX1 or KEA1 (Gaxiola et al., 1999; Maser et al., 2001), *Synechocystis* NhaS4 (Inaba et al., 2001), and *Escherichia coli* Kef-B (Booth et al., 1996). All these transporters have 10 to 12 membrane-spanning regions at the amino terminus and a carboxyl tail of variable lengths (Fig. 2A). AtCHX15 through AtCHX20, in particular, shared high identity and similarity with yeast KHA1, so AtCHX17 was chosen as a representative of this group (Fig. 1A).

Table 1. Predicted protein sizes of the entire CHX family in *Arabidopsis* and a summary of the gene expression patterns

Protein sequence was predicted either from the genomic sequence, full-length cDNA (+ from H. Sze, unpublished data; +R from Riken) or from both. Protein accession numbers are given for proteins that have either a cDNA or appear to be correctly predicted. Protein sequence with apparent annotation errors in the databases were revised (rev) by the Sze laboratory as shown in Supplemental Figure 1. The theoretical pI and molecular weight (Mw) of each protein was computed using the Compute pI/Mw tool at the Expert Protein Analysis System (ExPASy) Molecular Biology Server (<http://au.expasy.org/tools/pi_tool.html). RNA expression represents summary results from ATH1 genome array on pollen (Pol1), RT-PCR on mature pollen (Pol2), and from both approaches on SPR. SPR, Sporophytic tissues; a.a., amino acid; +, detection of an expression signal; -, no detectable signal; -/-, two independent results from microarray and RT-PCR of SPR, respectively (Figs. 3 and 4; Supplemental Table 1); nd, Not determined.

Gene Name	Accession Nos.		cDNA	Protein			RNA Expression		
	Locus	Protein		a.a.	Mw	pI	Pol1	Pol2	SPR
CHX01	At1g16380	AAD34690		785	88,908.78	6.31	+	nd	-/nd
CHX02	At1g79400	AAD30236	+	783	88,204.04	6.39	+	+	-/-
CHX03	At5g22900	BAB10611		822	92,452.77	7.50	+	+	-/-
CHX04	At3g44900	CAC03540		817	92,007.93	8.51	-	+	-/+
CHX05	At1g08150	NP_172294		815	91,606.19	6.56	+	+	+/-
CHX06a	At1g08140	BAC42972	+R	818	93,395.50	7.27	nd	+	nd/-
CHX06b	At1g08135			796 (rev)	90,112.28	7.01	nd	+	nd/-
CHX07	At2g28170			801 (rev)	90,989.71	7.29	-	+	-/-
CHX08	At2g28180		+	816 (rev)	90,956.09	7.22	+	+	-/-
CHX09	At5g22910	BAB10612		800	89,059.65	7.90	-	+	-/-
CHX10	At3g44930			783 (rev)	88,143.29	6.09	+	+	-/-
CHX11	At3g44920			783 (rev)	88,432.71	6.16	nd	+	nd/-
CHX12	At3g44910			770 (rev)	85,819.50	6.02	-	+	-/-
CHX13	At2g30240	AAM14917		831	92,189.42	6.03	+	+	-/-
CHX14	At1g06970	AAF82222	+	829	92,159.60	6.56	+	+	-/+
CHX15	At2g13620	NP_178985	+	821	89,859.54	5.71	++	+	-/-
CHX16	At1g64170			811 (rev)	88,050.60	8.82	-	-	+/+
CHX17	At4g23700	NP_194101	+	820	89,165.51	8.06	+	-	+/+
CHX18	At5g41610	BAB11467		810	87,383.34	8.71	+	+	+/+
CHX19	At3g17630	BAB02053		800	86,915.25	8.76	++	+	+/+
CHX20	At3g53720	AAO00889	+R	842	91,553.09	8.93	-	+	+/+
CHX21	At2g31910			832 (rev)	91,982.03	5.38	-	+	-/+
CHX23	At1g05580	AAL59981	+	867	95,867.43	6.02	+	+	-/-
CHX24	At5g37060	NP_198522		859	96,680.97	6.34	+	+	-/-
CHX25	At5g58460	NP_200654		857	95,833.29	8.32	+	+	-/-
CHX26	At5g01680	NP_195788		780	86,511.40	6.83	-	+	-/+
CHX27	At5g01690			767 (rev)	86,990.99	8.74	+	+	-/+
CHX28	At3g52080	AAM98175	+R	801	88,736.58	8.85	+	+	-/+

The hydrophilic carboxylic tail of CHX17 showed little identity with that of yeast KHA1 (10.9%), so the TM domain of selected AtCHX proteins was compared with those of CPA1 and CPA2 members. T-Coffee analyses showed that CHX02, CHX08, CHX13, CHX17, CHX28, and CHX25 clustered with yeast KHA1 (Fig. 2B; Supplemental Fig. 2). Although CHX08 and CHX25 showed less identity with KHA1, they shared more similarity (31%–34%) with KHA1 than with eukaryotic Na⁺/H⁺ exchangers (14%–19%). Several well-characterized Na⁺/H⁺ exchangers, including rat NHE1, AtNHX1 or SOS1/AtNHX7, yeast NHX1, and *Synechocystis* NhaS1 grouped in another clade, consistent with their classification as members of the CPA1 family. The amino-terminal region of CHX17 also showed slightly higher identity to AtKEAs (15.7%) than to AtNHX1 (12%). The TM domain of AtKEA1 shared high identity (38%) with *E. coli* K⁺ efflux transporters (Kef; Booth et al., 1996), suggesting AtKEAs may be functional homologs.

Interestingly, not only did the hydrophobic domain of AtCHX17 share high identity (32%) with that of yeast KHA1, it also had 35% identity with NhaS4 from the photosynthetic cyanobacterium *Synechocystis* PCC 6803 (Fig. 2, B and C). Putative TM region five (TM5) is particularly conserved among the three sequences, suggesting that this region participates in the transport of cation and H⁺ across the membrane. Twelve out of 23 residues are identical (52%), and 17 out of 23 residues are similar (74%). Many other predicted TMs (e.g. 6, 8, 9, and 12) also shared high (59%–69%) similarity. By contrast, TM5 regions of several Na⁺/H⁺ exchangers, including AtNHX1 and AtSOS1/NHX7, showed only 45% similarity with the TM5 of AtCHX17. *Synechocystis* NhaS4 is predicted to have 410 residues and approximately 12 TM spans. *E. coli* mutant T0114 expressing NhaS4 did not show Na⁺/H⁺ antiport activity. However, those cells were tolerant to K⁺-depleted conditions, suggesting NhaS4 might transport K⁺ (Inaba et al., 2001). Yeast KHA1 is a putative K⁺/H⁺ exchanger, as *kha1* disruption

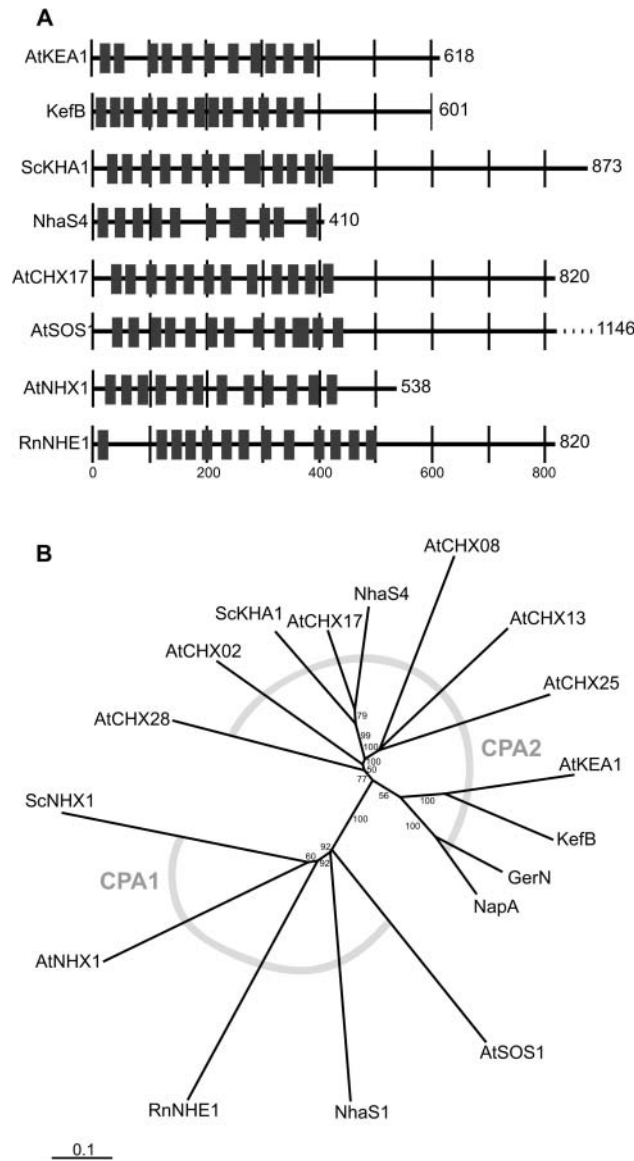


Figure 2. AtCHX proteins share similarity with a putative K^+/H^+ antiporter from yeast. **A**, Members of the CPA superfamily have an amino-terminal hydrophobic domain and a hydrophilic tail of variable lengths. This scaled graphic representation of the TM regions for the selected protein sequences was created using information compiled from the Simple Modular Architecture Research Tool site (<http://smart.embl-heidelberg.de>). Each gray bar corresponds to a TM region of 17 to 22 amino acids. Accession numbers are RnNHE1, rat P26431; AtSOS1/AtNHX7, At2g01980; AtNHX1, At5g27150; KefB, *E. coli* AAC76375; ScKHA1, yeast P40309; NhaS4, *Synechocystis* PCC 6803 slr1595 or NP_440311; AtKEA1, At1g01790; and AtCHX17, At4g23700. Total residue number is given at the end of each protein. **B**, AtCHX proteins cluster with yeast KHA1, and *Synechocystis* NhaS4 in phylogenetic analyses of the TM domain. The hydrophobic domains, including the first Met to the end of the last TM span, from several cation/proton exchangers were aligned. This unrooted phylogenetic tree was created by using the multiple sequence alignment computed by the program T-Coffee, version 1.42. Values shown indicate the number of times (in percent) that each branch topology was found in 1,000 replicates of the performed bootstrap analysis using PAUP*, version 4.0b10. Accession numbers are RnNHE1, rat P26431; AtSOS1, *Arabidopsis* At2g01980; AtNHX1, At5g27150; KefB, *E. coli*, AAC76375; ScKHA1, yeast P40309; ScNHX1, NP_010744; NhaS4 and NhaS1, *Synechocystis* PCC 6803 slr1595 or NP_440311 and NP_441245; AtKEA1, At1g01790; GerN, *B. cereus* AAF91326; and NapA, *E. hirae* P26235. Accession numbers of AtCHX02, 08, 13, 17, 25, and 28 are in Table I. **C**, The TM domain of AtCHX17 or OsCHX13 shares high identity with that of ScKHA1 and *Synechocystis* NhaS4. The TM domain of AtCHX17 (At4g23700), OsCHX13 (TIGR ID 3571.m00152), and ScKHA1 (P40309), including residues 1 to 427, 1 to 415, and 1 to 428, respectively, were aligned with the entire *Synechocystis* NhaS4 (NP_440311) of 410 residues using T-Coffee, version 1.83. TM5 is particularly conserved with 54% (77%) identity (similarity). Identical or similar residues are blocked as dark or light boxes, respectively. Gray underline marks the approximate TM region. ●, Conserved residues in all CHX proteins; ◇, residues conserved in all CHX and in CPA1 shown in B.

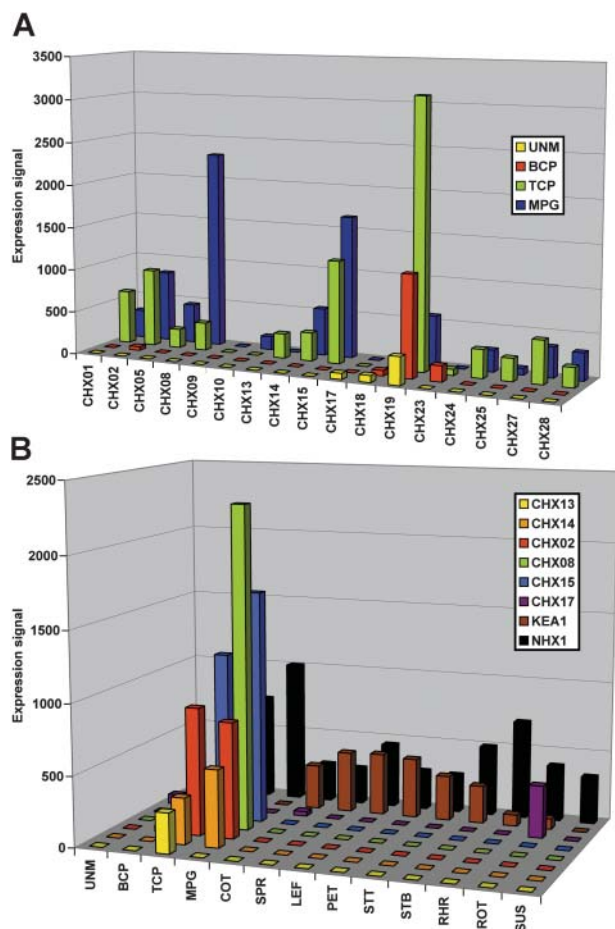


Figure 3. Many *AtCHX* genes are preferentially expressed in the male gametophyte according to whole-genome ATH1 microarray. A, *AtCHX* genes are differentially expressed during microgametogenesis. RNA isolated from microspores (UNM), bicellular pollen (BCP), tricellular pollen (TCP), or mature pollen (MPG) was used for microarray hybridization. Data represent the mean signal of two independent experiments that showed reliable expression signals (Supplemental Table I). B, Multiple Arabidopsis *CHX* genes show pollen-specific expression, whereas *KEA1* and *NHX1* are highly expressed in sporophytic and gametophytic tissues. Gene expression in pollen was compared with that in sporophytic tissues, including cotyledons (COT); leaves (LEF); whole sporophyte (green tissues) at rosette stage (SPR); petioles (PET); stem, top (STT); stem, base (STB); root hair zone (RHR); roots (ROT); and suspension cell cultures (SUS; Supplemental Table I). The same amount of total RNA was used in all Affychip hybridizations. Data represent normalized mean of two to three datasets, except for data of SPR, which came from four replicates.

Figure 5, A and B, the GUS expression driven by the 715-bp *AtCHX08* promoter and the 979-bp *AtCHX23* promoter was found in pollen. Like *AtCHX08*, *AtCHX13* expression was not detected in vegetative tissues, and in mature plants, GUS activity was only observed within the anthers of flowers (Fig. 5D).

To identify cell types expressing GUS, flowers were sectioned. *CHX13::GUS* expression was observed in pollen both before and after germination. GUS staining was detected in pollen grains within anthers of the flower buds or in pollen on fully open flowers (Fig. 5E)

and on the stigma, and in pollen tubes growing in the style (Fig. 5F). In some anther cross-sections, the endothecium and epidermis showed blue staining (data not shown). In mature plants expressing the reporter driven by the 778-bp *AtCHX14* promoter, GUS signals were seen in the pollen (Fig. 5G) but also in all parts of flowers (data not shown), which is significantly different from that in *AtCHX13::GUS* transgenic lines. The *AtCHX14* reporter was also expressed in young leaf tissues, particularly in the basal cells of trichomes (Fig. 5H) and in the vascular tissues of roots (Fig. 5I).

While *AtCHX14* appears to be expressed in pollen and vegetative tissues, the reporter from the 2-kb promoter of *AtCHX17* was expressed predominantly in epidermal and cortical cells of mature root (Fig. 5C). Interestingly, GUS expression was detected along the mature root but not the root tip, consistent with a microarray study of root cell types at different developmental stages (Birnbaum et al., 2003). In addition to the roots, *CHX17::GUS* activity was also observed in anthers, consistent with the microarray data from uninucleate microspores (Fig. 3B). *CHX17::GUS* activity was barely detected in leaves (Cellier et al., 2004), although RT-PCR showed weak expression in rosette leaves (Fig. 4).

In general, all of the GUS reporter results are consistent with the expression patterns we observed using RT-PCR (Fig. 4) and with the microarray data from pollen (Fig. 3; Becker et al., 2003; 8K GeneChip, Honys and Twell, 2003) and roots (Birnbaum et al., 2003). Therefore, the chimeric reporter genes were good markers of *AtCHX* transcript localization. Moreover, the ATH1 microarray data of developing pollen are remarkably reliable. Occasional quantitative differences between RT-PCR and microarray signals (Table I) may result from differential sensitivities of the two approaches or from normalization of the microarray data that eliminated weak signals.

Fewer *CHX* Genes in Rice Suggests Diversification of *CHX* in Arabidopsis

As a step to understand *CHX* function in plants, we searched for rice *CHX* genes using TBLASTN (Altschul et al., 1997). Many BAC or PAC clones were not yet annotated; however, 28,000 full-length cDNA sequences are available from rice (Kikuchi et al., 2003). Thus, genomic DNA sequences and predicted proteins from either The Institute for Genomic Research (TIGR; <http://www.tigr.org/tdb/e2k1/osa1/index.shtml>) or Aramemnon (<http://aramemnon.botanik.uni-koeln.de>) sites were verified with cDNA and translation products, respectively, whenever possible (Tables II and III). OsCHX proteins are predicted to range from 780 to 875 residues, with a hydrophobic amino-terminal domain. However, one protein, OsCHX11, has only 453 residues and does not have a hydrophilic domain at the carboxylic terminus. Phylogenetic analysis of rice *CHX* proteins was conducted using

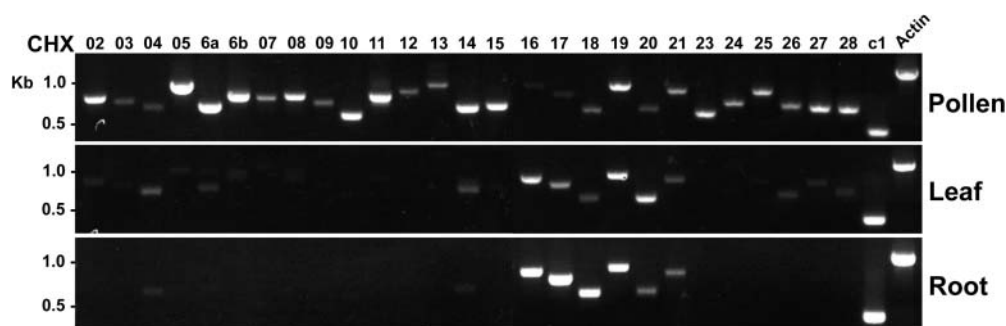


Figure 4. RT-PCR demonstrates additional *AtCHX* genes expressed in pollen, including CHX3, 4, 5, 6a, 6b, 11, and 12. RNA (1 μ g) isolated from mature pollen, leaf, or root of wild-type *Arabidopsis* plants (ecotype Columbia) was reverse transcribed to cDNA. Each CHX gene was amplified for 35 cycles of 94°C for 30 s, 55°C for 30 s, and 72°C for 90 s. Amplified products came from cDNA as their sizes were similar to the predicted length, and one-half of the primer sets spanned an intron (Supplemental Table II). Actin 11 (At3g12110) and *VHA-c1* (At4g34720) fragments amplified by PCR are 1,130 and 482 bp long, respectively. Result is representative of two to three experiments.

T-Coffee (Supplemental Fig. 3) and, based on their relationship to one another, we have named them OsCHX01 to OsCHX17.

Several OsCHX proteins were highly conserved with *AtCHX* proteins (Fig. 6; Supplemental Fig. 4). In clade I, OsCHX4 shared 47% similarity to *AtCHX28*. OsCHX01 and OsCHX02 shared 42% to 44% similarity to *AtCHX01*. Both OsCHX01 and OsCHX02 cDNAs were detected in a flower library (KOME site; <http://cdna01.dna.affrc.go.jp/cDNA>), suggesting they may be expressed like their *Arabidopsis* counterparts in pollen. In clade IV, *AtCHX20* shared 66% similarity to OsCHX12. OsCHX16 and OsCHX17 shared 61% to 63% similarity with *AtCHX15*. Three rice CHX proteins (OsCHX13–OsCHX15) shared 69% to 73% similarity with *AtCHX19*, suggesting that these are functional orthologs. *AtCHX19* is particularly interesting because its expression is high in bicellular and tricellular pollen, but transcripts decreased in mature pollen (Fig. 3A). These results indicate that multiple *CHX* genes played roles in plants long before the separation of monocots and dicots.

However, a 40% reduction in rice *CHX* genes relative to *Arabidopsis* is surprising. It is caused by the absence of rice orthologs in clades II and III of *Arabidopsis* (Figs. 1A and 6). These two branches include 15 *AtCHX* proteins (03–14, 26, and 27), all of which are preferentially expressed in pollen. This finding suggests a diversification of *CHX* genes in *Arabidopsis*, although the significance of so many copies is unclear.

DISCUSSION

Bioinformatic Analyses of a Novel *CHX* Family from Rice and *Arabidopsis*

Here, we present the first bioinformatic analyses of a novel gene family, *CHX*, encoding putative

cation transporters in plants, to provide a strong foundation and working ideas to test their functions. We show that all 28 *AtCHX* proteins are remarkably similar in size (Table I), contrary to an initial report based on database annotations (Maser et al., 2001). Until all full-length cDNAs are sequenced, parts of Table I (Supplemental Fig. 1) and Table III (Supplemental Fig. 3) are considered best protein predictions. The amino-terminal domains of 28 *AtCHX* and 16 OsCHX proteins consist of 10 to 12 TM spans (approximately 430 residues), and a hydrophilic carboxylic-terminal domain of ≥ 360 residues. The hydrophobic domain, including TM5 and TM6, of *AtCHX16* to *AtCHX19* and OsCHX13 to OsCHX15 are especially conserved relative to yeast KHA1 (Ramirez et al., 1998) and *Synechocystis* NhaS4 (Inaba et al., 2001; Fig. 2C), suggesting that they participate in the transport of K^+ (Na^+) and H^+ as discussed below.

Surprisingly, many *AtCHX* genes are preferentially expressed in pollen. We demonstrated this (Figs. 3–5) using whole-genome microarray of developing pollen, RT-PCR of pollen message, and promoter-driven GUS-reporter staining of plants. To our knowledge, no other transporter families, including PM (AHA) or vacuolar H^+ pumps (VHA), Ca^{2+} pumps (ACA, ECA), aquaporins (AQP), other cation/ H^+ cotransporters (KEA, CAX, NHX, KUP), and K^+ /ion channels (KAT, AKT, KCO, CNGC) show a comparable proportion of pollen-specific or preferential expression (data not shown; Becker et al., 2003; Honys and Twell, 2003). Strikingly, rice has roughly half as many *CHX* genes as *Arabidopsis*. Phylogenetic analyses show that rice is reduced in the number of *AtCHX* orthologs that are expressed in pollen. The extra *CHX* genes in *Arabidopsis* may suggest redundant functions. Alternatively, we speculate that pollen development, survival, and germination in *Arabidopsis* may differ from rice with regard to cation transport requirements.

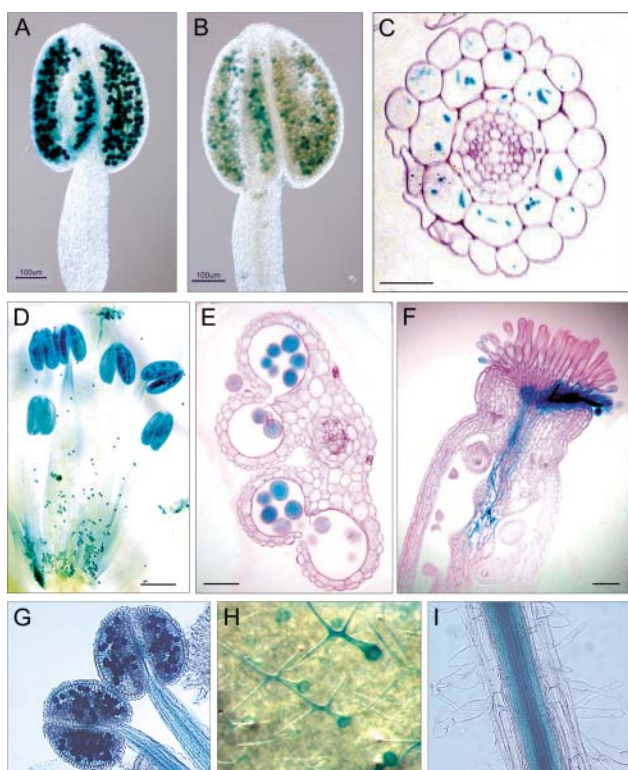


Figure 5. Promoter::GUS activity shows *CHX* expression in pollen and in vegetative tissues of transgenic Arabidopsis plants. *AtCHX08::GUS* (A) and *AtCHX23::GUS* (B) expression in pollen grains. GUS activity was detected after an overnight reaction period in mature flowers from 6-week-old T1 transgenic plants harboring either a 715-bp *AtCHX08* or a 979-bp *AtCHX23* promoter region fused transcriptionally to GUS. Scale bars = 100 μm . C, *AtCHX17::GUS* expression in epidermal and cortical cells of root. GUS-staining signals were detected in roots, but not leaves, of 6-week-old transgenic Arabidopsis plants harboring the 2.0-kb *AtCHX17* promoter region transcriptionally fused to GUS. Scale bar = 50 μm . D to F, *AtCHX13::GUS* expression in reproductive organs. GUS staining was only seen in anthers and pollen grains of mature flowers from 6-week-old transgenic Arabidopsis plants harboring the 2.0-kb *AtCHX13* promoter region transcriptionally fused to GUS. D, Whole flower; E, transverse section of anthers; F, longitudinal section of stigma showing growing pollen tubes expressing *AtCHX13::GUS*. Scale bar represents 400 μm (D), and 50 μm (E and F). G to I, *AtCHX14::GUS* expression in flowers and vegetative tissues. GUS-staining signals were detected in whole flowers (including anthers and pollen grains) from 6-week-old plants (G), leaf trichomes (H), and root vascular tissues (I) from 20-d-old transgenic Arabidopsis plants harboring the 774-kb *AtCHX14* promoter region transcriptionally fused to GUS. Images in G to I are magnified seven times.

Members of the CPA Superfamily Have Various Transport Modes

CPA1 in Plants and Animals Catalyze K^+/H^+ and Na^+/H^+ Exchange

What is the transport function of related CPA members? Although AtNHX1 and AtSOS1 (AtNHX7) are best known as Na^+/H^+ exchangers (Apse et al., 1999; Qiu et al., 2002), recent studies have shown that members of the NHX family show differential cation

specificities. A purified Arabidopsis NHX1 reconstituted in liposomes transported K^+ and Na^+ equally well (Venema et al., 2002). Moreover, a prevacuolar Golgi-associated LeNHX2 reconstituted in liposomes catalyzed K^+/H^+ exchange better than Na^+/H^+ exchange (Venema et al., 2003). The tomato NHX2 may be an ortholog of AtNHX5 (At1g54370) or AtNHX6 (At1g79610), as they share 75% identity (82% similarity). That study provided the first molecular evidence for an intracellular K^+/H^+ exchanger in plants.

Physiological and phylogenetic observations support the idea that the *in vivo* activity of plant NHX is to exchange K^+ for H^+ : (1) Unlike animal cells, which maintain a steep Na^+ gradient across the PM, plant cells are not usually exposed to high Na^+ , and thus $[\text{Na}^+]_{\text{cyt}}$ levels are low; (2) K^+ is the major osmoticum of all eukaryotes and is maintained at 75 mM or higher in the cytosol of plants (Walker et al., 1996); and (3) plant NHX proteins catalyze K^+/H^+ or Na^+/H^+ exchange (Venema et al., 2002) and, in some cases, K^+ is preferentially transported over Na^+ (Venema et al., 2003). In mammals, intracellular membrane-associated NHE7 mediates the influx of K^+ or Na^+ in exchange for H^+ (Numata and Orłowski, 2001). ^{86}Rb influx into the endomembrane compartment of permeabilized CHO cells expressing NHE7 was reduced by K^+ , Na^+ , or Li^+ . Results indicate that NHE7 is a nonselective monovalent cation/ H^+ exchanger. Given that K^+ is the major ion in all eukaryotic cells, the physiologically relevant activity of many plant intracellular NHXs and that of animal endomembrane NHE is most likely K^+/H^+ exchange.

Prokaryotic and Yeast CPA2 Behave as Cation/ H^+ Exchanger and as Ion Channel

In addition to AtCHX, the CPA2 family in Arabidopsis includes six KEA genes of unknown function (Maser et al., 2001). Three (KEA1–KEA3) proteins share approximately 31% identity to bacterial KefC or KefB transporters (Fig. 2B). KefB- or KefC-mediated K^+ efflux in *E. coli* is activated by adducts of glutathione and negatively regulated by glutathione, so they are proposed to function in survival of stress, resulting from damage caused by electrophilic sulfhydryls, such as *N*-ethylmaleimide (Booth et al., 1996). Initially thought to function as K^+/H^+ antiporters, KefB or KefC behave like ligand-gated ion (K^+ efflux) channels and share structural similarities with K^+ channels (Booth et al., 1996; Ferguson et al., 1997; Miller et al., 1997). Several K^+ channels and KefC possess a K^+ -transport, nucleotide-binding motif, suggesting conservation in the ligand sensor mechanism controlling the gate (Roosild et al., 2002). The carboxyl-terminal domain of KEA1 (residues 422–536), KEA2, and KEA3 shares high similarity to KefC or KefB, suggesting that plant KEAs might be ligand-gated ion channels.

However, NapA from *Enterococcus hirae* (CPA2) was reported to encode a Na^+/H^+ antiporter based on

Table II. *The japonica rice genome has only 17 CHX genes*

The genes were numbered according to the phylogenetic relationship of the protein sequences (see Table III). The position of the start and stop codon on the BAC or PAC clones is indicated as either on the forward or on the reverse [–] strand. The first ATG was located in the first exon in all cases. The TIGR gene ID number is provided for future identification, as the UniGene cluster number was unavailable. Chr, Chromosome number.

OsCHX	Chr	BAC/PAC Clone	Accession No.	Position ATG-STOP	Exon No.	TIGR Gene ID
01	2	OJ1282_E10	AP005290	56,676–59,266	2	4910.t00011
02	8	OSJNBb0011H15	AP005251	8,972–11,696	4	7208.t00002
03	9	P0705E11	AP006548	[–] 116,417–113,865	2	8149.t00015
04	12	OSJNBa0063N15	AL732378	73,678–76,155	1	5720.t00016
05	5	P0486C01	AC135924	38,925–41,773	3	6388.t00005
06	12	OSJNBa0024J08	BX000492	[–] 56,984–54,565	2	6559.t00011
07	11	OSJNBa0010K05	BX000497	141,611–144,016	1	6554.t00032
08	8	P0470F10	AP004562	137,679–140,243	2	3508.t00006
09	12	OJ1311_G04	BX000506	12,549–15,153	2	7236.t00003
10	11	OSJNBa0074L01	AC136970	85,198–87,751	2	7498.t00017
11	5	OSJNBa0088M05	AC136222	[–] 128,439–124,482	3	6422.t00020
12	5	OSJNBb0041A22	AC093921	25,581–29,615	3	7450.t00007
13	3	OSJNBa0010E04	AC096687	[–] 27,131–22,453	2	3571.t00006
14	5	P0692E03	AC130731	8,097–10,588	2	5816.t00003
15	12	OJ1388_B05	BX000457	96,921–102,797	2	7234.t00016
16	5	OSJNBb0099O15	AC118289	[–] 87,192–84,471	2	4376.t00012
17	1	P0454H12	AP003255	40,971–43,842	4	2814.t00007

inability of *napA* mutants to grow on Na⁺-rich medium and reduced Na⁺/H⁺ antiport activity in isolated vesicles (Waser et al., 1992). GerN, a protein that is needed for *Bacillus cereus* spore germination, complemented Na⁺ sensitivity of an *E. coli* mutant, suggesting that GerN has Na⁺/H⁺ antiport activity. However, GerN also used K⁺ as a coupling ion, as intravesicular K⁺ stimulated ²²Na⁺ uptake by everted vesicles (Southworth et al., 2001). These studies are

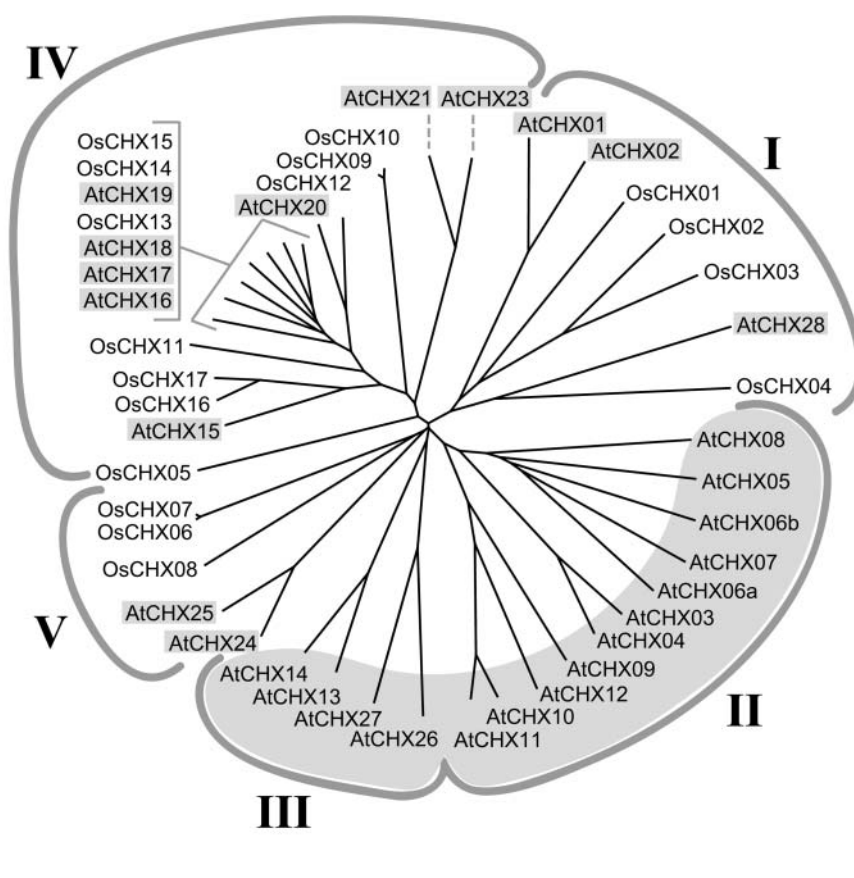
consistent with a model for Na⁺/H⁺-K⁺ antiport, where K⁺ enters the cell. GerN is proposed to have a physiological role in K⁺ acquisition and pH homeostasis (Southworth et al., 2001). Interestingly, the yeast KHA1 is thought to extrude K from the cell by K⁺/proton exchange, as the *kha1* mutant has increased K⁺ content (Ramirez et al., 1998). However, an *E. coli* mutant, expressing NhaS4 from *Synechocystis*, is tolerant to K⁺-depleted medium, suggesting NhaS4

Table III. *All OsCHX proteins are predicted to have 780 to 875 residues except for OsCHX11, which lacks the hydrophilic domain at the carboxyl terminus*

Protein sequences were predicted from either genomic DNA, full-length cDNA, or both. cDNAs were obtained from a flower or callus library as indicated (KOME Web site). The proteins were named OsCHX and numbered according to their phylogenetic relationship. A few sequences were revised (rev). TIGR and Aramemnon ID numbers provide a reference for annotation purposes. Chr, Chromosome number; a.a., amino acid; Mw, molecular weight.

OsCHX	Chr	Accession Nos.		Protein			TIGR Protein ID	Aramemnon ID	Library
		cDNA	Protein	a.a.	Mw	pI			
01	2	AK100456		830 (rev)	88,690.80	6.43	4910.m00124	Os02.8351.m05651	Flower
02	8		BAD10196	817	87,826.96	6.93	7208.m00097	Os08.8356.m04259	
03	9	AK069882		827	88,975.00	6.21	8149.m00120	Os09.8357.m03100	Flower
04	12			825	88,694.15	6.56	5720.m00111	Os12.8359.m04248	
05	5	AK100933		834 (rev)	89,676.56	8.78	6388.m00147	Os05.8353.m03499	Flower
06	12			801	85,569.52	6.75	6559.m00134	Os12.8359.m00082	Flower
07	11	AK100300		801	85,635.71	6.75	6554.m00181	Os11.8358.m00082	
08	8	AK100696	BAD09470	825	88,680.29	6.33	3508.m00228	Os08.8356.m00141	Flower
09	12	AK072782		839	89,046.43	6.30	7236.m00090	Os12.8359.m00182	Flower
10	11			822	87,230.37	6.43	7498.m00133	Os11.8358.m00205	
11	5			453	46,152.79	8.64	6422.m00166	Os05.8353.m02754	
12	5	AK106443	AAS75243	844	89,690.30	7.16	7450.m00125	Os05.8353.m00128	Callus
13	3	(NM_185113)	AAL79755	780	82,322.00	8.84	3571.m00152	Os03.8360.m05537	
14	5	AK069092		790	84,937.39	7.02	5816.m00077	Os05.8353.m01666	Flower
15	12			802	85,625.58	9.27	7234.m00133	Os12.8359.m04033	
16	5	AK106318		874	93,260.23	6.69	4376.m00176	Os05.8353.m03605	Callus
17	1		BAB62576	875	94,904.54	6.34	2814.m00132	Os01.8350.m05627	

Figure 6. Arabidopsis CHX are orthologous to rice CHX, except for a clade of 15 AtCHX. Accession and identification numbers for Arabidopsis and rice proteins are listed in Tables I and III, respectively. The full revised protein sequences from Arabidopsis and rice were aligned using T-Coffee, version 1.83, and PAUP*, version 4.0b10, was used for bootstrap analysis. The number of times (in percent) that each branch topology was found in 1,000 replicates of the performed bootstrap analysis for clades I, II and III, IV, and V are 63%, 81%, 53%, and 98%, respectively.



facilitates K^+ uptake (Inaba et al., 2001). Together, these results suggest that members of the CPA2 family have various catalytic modes.

Working Models for Cation/Proton Exchanger Function in Plant Cell Biology

If most plant NHXs and KEAs are K^+ (Na^+) transporters, what is the role of additional CHX-like proteins? *NHX* (Yokoi et al., 2002) and *KEA* genes are expressed widely in vegetative tissues as well as in the male gametophytes, according to ATH1 genome array results (Fig. 3; Supplemental Table I). Here, for simplicity, we consider CHX as K^+ (Na^+)/ H^+ antiporter, although various transport modes (e.g. K^+ / Na^+ exchange) are considered for members of the family. An exchange mechanism requires reciprocity in transport behavior and, thus, two modes are possible: Energetically, a downhill movement of a proton could drive K^+ flux; however, it is also possible that K^+ movement down its gradient is coupled to H^+ flux uphill. If so, these transporters could induce rapid changes in the osmotic potential and the pH across a membrane. Physiological studies and thermodynamic considerations indicate a need for K^+ / H^+ exchangers on the mitochondria, chloroplast, PM, and intracellular membranes of the secretory system.

Plants have a remarkable ability to maintain cytosolic K^+ homeostasis under either K^+ -replete or K^+ -depleted conditions. When external K^+ is low or deficient (0–0.1 mM), cells maintain a $[K^+]_{\text{cyt}}$ of about 66 to 75 mM, probably by increasing uptake via K^+ / H^+ symport and by redistributing K^+ from other compartments, including the vacuole. When external K^+ is in excess (5 mM), the $[K^+]_{\text{cyt}}$ is unchanged, and excess K^+ is stored in the vacuole (Walker et al., 1996). Under these conditions, thermodynamic calculations support a model for active sequestration of K^+ in the vacuole and extrusion of K^+ out of the cell at the PM. Active transport could be mediated by K^+ / H^+ exchangers fueled by the proton electrochemical gradient across the vacuolar membrane and the PM. Conceivably, K^+ (Na^+)/ H^+ antiporters, like *NHX1* and *CHXs*, could fill this role to maintain K^+ homeostasis in the cytosol and regulate pH_{cyt} . Mitochondria or plastids, like prokaryotes, also need to maintain adequate $[K^+]$ in the matrix or stroma to support enzyme activities needed in respiration or in photosynthesis. With an electric potential negative inside (-100 mV or more) in mitochondria, K^+ is taken up passively. To regulate organelle volume, excess K^+ may be extruded by a K^+ / H^+ exchanger as in rat liver mitochondria (Martin et al., 1984). Photosynthetic CO_2 uptake in isolated chloroplasts is enhanced when external K^+ is approximately

100 mM. A K^+/H^+ counterflow at the chloroplast envelope was suggested to bring K^+ in and move H^+ out to maintain a basic pH in the stroma during illumination (Wu and Berkowitz, 1992). The molecular identities of these exchangers on the mitochondria or plastids are unknown. NHXs, KEAs, and CHXs are potential candidates.

Recent studies highlight roles of C^+/H^+ exchangers in protein sorting and vesicular transport. First, yeast Nhx1p and human NHE6 and NHE7 have been localized to prevacuolar/vacuolar compartments, recycling endosomes and the Golgi network, respectively (Nass and Rao, 1998; Numata and Orlowski, 2001; Brett et al., 2002). Second, genetic evidence showed that $\Delta nhx1$ mutants missorted vacuolar proteins, indicating that NHX1 is needed for protein trafficking (Bowers et al., 2000). Although the mechanism is unclear, it is conceivable that NHX1 or related cation/ H^+ exchangers could affect the osmolarity, volume, and pH of intracellular compartments. The acidic pH may be required for the maturation and processing of secreted proteins, for the dissociation and recycling of endocytosed materials, and for protein-protein association and dissociation of regulated vesicular trafficking (Ali et al., 2004). In the Japanese morning glory, a mutation in *nhx1* produced purple, instead of blue, open flowers (Yamaguchi et al., 2001). The vacuolar pH was more acidic in the mutants, indicating that NHX1 has a critical role in regulating lumenal pH. It is possible that CHX proteins are also involved in pH regulation and vesicular trafficking.

Potential Roles of CHX in Pollen Development, Survival, and Tube Growth

Why are so many CHX genes preferentially or specifically expressed during male gametogenesis in Arabidopsis? The development of male gametophytes, pollen germination, and pollen tube growth is tightly regulated to ensure successful delivery of male gametes to the ovule within a short time. This requires a major contribution of a gametophytic gene expression program (Twell, 2002; Honys and Twell, 2003; this study). It is likely that CHX proteins are involved in one or more of the following events integral to microgametogenesis and pollen tube growth: expansion of the microspore that is associated with the generation and fusion of numerous small vacuoles to form a single, large vacuole; vacuole fission to form multiple smaller vacuoles during vegetative cell maturation; dehydration of the pollen cytoplasm during final pollen maturation; rehydration of pollen during germination; formation and maintenance of new vacuoles during pollen germination; and polarized pollen tube growth (Twell, 2002).

Clearly, there is an abundance of transport activities associated with pollen development and tube growth. These include ion and metabolite transport, vacuole formation, osmotic adjustments during dehydration and rehydration, vesicular trafficking, secretion of extracellular materials, and endocytosis to recycle

proteins (Hepler et al., 2001). Furthermore, pollen tubes not only maintain a high $[Ca^{2+}]$ as well as $[H^+]$ gradient, at the extreme apex, growth is accompanied by influx of Ca^{2+} , H^+ , and K^+ at the tip and H^+ efflux at the base of the clear zone (Feijo et al., 1999; Messerli et al., 1999). Such ion currents are a result of the specific placement of transporters at the tip or base of the pollen tube (Feijo et al., 2001; Holdaway-Clarke and Hepler, 2003). The discovery of pollen-specific transporters (Schwacke et al., 1999; Mouline et al., 2002; Scholz-Starke et al., 2003; this study) is consistent with the special needs of pollen development, although the multiplicity of CHX expressed in pollen is unprecedented among transport families.

An intriguing phenomenon is that dehydration sets in as male gametophytes reach maturity. Several genes up-regulated in vegetative tissues by salt or dehydration stress are also expressed in pollen of unstressed plants, suggesting a need to make osmotic adjustments during microgametogenesis (Yoshida et al., 1999). An increase in the CHX19 message during the uninucleate microspore and bicellular pollen (Fig. 3) suggests a role for this cation/proton exchanger at an early phase of male gametogenesis, perhaps associated with vacuole morphogenesis, whereas other CHX messages (CHX15 and CHX8) peak in the tricellular or mature pollen (Fig. 3A; Supplemental Table I) and could be associated with osmotic adjustment during dehydration and/or pollen germination following rehydration. It is interesting that *AtCHX17* transcript level is increased 4- to 8-fold in roots in response to high salt or abscisic acid (Kreps et al., 2002; Cellier et al., 2004). Furthermore, K^+ content in roots of *Atchx17* mutants is decreased (Cellier et al., 2004), indicating CHX17 affects net K^+ uptake. Together, the results support a model that *AtCHX17* has a role in regulating K^+ homeostasis and in stress protection.

This study further highlights the potential regulatory role of the carboxyl domain of CHX in rice and in Arabidopsis. Interestingly, the hydrophilic domains of *AtCHX*, in general, share 34% to 52% similarity with one another, and up to 84% to 94% similarity for products of gene duplication. Several highly conserved regions stand out in rice and Arabidopsis (Supplemental Fig. 4), such as residues 636 to 645 (FXGGXDDREA) in CHX17, suggesting they interact with similar motifs or molecules. Development of male gametophyte and pollen tube growth are subject to posttranslational regulation by the environment and signaling molecules in the transmitting tissue (Hepler et al., 2001; Holdaway-Clarke and Hepler, 2003), so the hydrophilic domains of CHX may be involved in osmosensing and/or transducing signals to promote osmotic adjustments and polarized growth. It is possible that CHXs are involved in local small-scale ion movement rather than bulk ion movement. Experiments to determine transport activity and regulation, membrane location, and biological roles of *AtCHX* proteins are in progress. Resources generated from these studies, including mutants and cDNAs, will

be announced (<http://www.life.umd.edu/CBMG/faculty/sze/lab/2010.html>) and available to the community to understand how this large group of CHXs is integrated with plant growth, reproduction, and survival.

MATERIALS AND METHODS

Plant Materials and Growth Conditions

Arabidopsis ecotypes Columbia (Col-0), Landsberg *erecta* (*Ler*), and Wassilewskija (Ws) were used in this study. Wild-type and transgenic seeds were sterilized according to published procedures (Boyes et al., 2001; Cheng et al., 2003). Plants were grown in a variety of locations under varying growth conditions. In general, growth conditions in the light incubators were as follows: 16-h-light/8-h-dark cycles, light intensity $150 \mu\text{mol s}^{-1} \text{m}^{-2}$ photosynthetically active radiation, temperature $22^\circ\text{C}/20^\circ\text{C}$. In the greenhouse, plants were grown on compost (Neuhaus Humin Substrat N2; Klasmann-Deilmann, Geeste, Germany) and subirrigated with tap water. Greenhouse growth conditions were as follows: 16-h-light/8-h-dark cycles, sunlight intensity limited to $300 \mu\text{mol s}^{-1} \text{m}^{-2}$ photosynthetically active radiation, temperature $25^\circ\text{C}/24^\circ\text{C}$.

Construction of Promoter::GUS Reporters

To examine the precise gene expression, each *AtCHX* (such as *CHX08*, *CHX13*, *CHX14*, *CHX17*, or *CHX23*) gene promoter region upstream of the ATG start codon was transcriptionally fused with GUS to generate the *CHX*::GUS reporter.

To make *CHX08* and *CHX23* GUS fusion constructs, promoter fragments of those two genes were amplified by PCR from Col-0 genomic DNA isolated from 3-week-old seedlings using the Expand High Fidelity PCR system (Roche, Mannheim, Germany). The primers used to generate the 715-bp *CHX08* promoter region were 5'-CGCGTCGACGGCTGCTATGTTT-GACGTTTGAG-3' (appended *SalI* site is underlined) and 5'-CGCGGATCC-GACTTCAAATCTTAAGTGAGTTCCTG-3' (*BamHI* site is underlined). The primers used to generate *CHX23* (979 bp) are 5'-CGCGTCGACGCTA-CACTCCTAGATCAGAGTAAACAAG-3' (appended *SalI* site is underlined) and 5'-CGCGGATCCCTCCTACGATGGCTGGTCGGAATCCC-3' (appended *BamHI* site is underlined). The *SalI*-*BamHI* PCR fragments of *CHX08* and *CHX23* promoters were cloned into the same sites of the plasmid pRITA I (Eshed et al., 2001) to make the transcriptional reporter fusion, resulting in pCHX08-RITA and pCHX23-RITA, respectively. Promoter fragments were verified by sequencing. The GUS fusion cassettes for *CHX08* and *CHX23* were released by *NotI* from pCHX08-RITA and pCHX23-RITA, then subcloned into the same site of the binary vector, pMLBart (Gleave, 1992), resulting in *CHX08*::GUS and *CHX23*::GUS constructs.

For making transcriptional fusion of *CHX13* and *CHX17* with GUS, a 2-kb fragment corresponding to the *CHX13* and *CHX17* promoter region was amplified by PCR using the following primers: forward primer 5'-TTTT-CCATGGCTTTTCTTATCAGTAAAACG-3' and reverse primer 5'-TTT-GGATCCGGCTTGTTTTGTCTTGTACTTG-3' for *CHX13*; and forward primer 5'-TTTTCCATGGTTTAAAGATCTGACAAATGATGAATATG-3' and reverse primer 5'-TTTTGGATCCTCTACCTGAGTTTGTTTAAACC-3' for *CHX17*. A unique *NcoI* site at the ATG initiation codon of the *CHX13* and *CHX17* coding sequence and a *BamHI* site at the 5' end of the gene were introduced (underlined). The PCR products were digested with *NcoI* and *BamHI*, and the resulting fragment was cloned into pBi320.X (provided by R. Derose, RhoBio, Evry, France) leading to a transcriptional fusion between the *CHX13* promoter region and the GUS coding sequence. pBi320.X bears a unique *NcoI* site at the initiation codon of a promoterless GUS coding sequence located upstream of the nopaline synthase terminator. The *CHX13* and *CHX17* promoter sequences of the construct were verified by sequencing, and the corresponding complete expression cassettes were subcloned into a pMOG 402 binary vector (H. Hoekema, MOGEN International, Leiden, The Netherlands), resulting in *CHX13*::GUS and *CHX17*::GUS.

To generate the *CHX14*::GUS construct, the *CHX14* promoter region was amplified by PCR using a forward primer 5'-GGCAAGCTTGAGTTTTGT-TATCGGATGAAT-3' and a reverse primer 5'-CGGGGATCCCTCTG-CATCGAGTTACCTCCTCCGA-3'. The restriction enzyme sites *HindIII* and *BamHI* were introduced (underlined). The *CHX14* (778-bp) promoter PCR

product was cloned into pGEM-T (Promega, Madison, WI) and verified by sequencing. *CHX14* promoter fragments were subcloned into the *HindIII*/*BamHI* sites of pBI121 to replace the cauliflower mosaic virus 35S promoter and generate the chimeric *CHX14*::GUS construct.

All the recombinant plasmids were transformed into *Agrobacterium tumefaciens* GV3101 (Koncz and Shell, 1986; Sambrook et al., 1989). These strains were used to transform *Arabidopsis* ecotype Columbia using the floral dip method (Clough and Bent, 1998). Transgenic progenies were selected either on one-half strength Murashige and Skoog standard medium, supplemented with 25 to 50 μg kanamycin (for *CHX13*::GUS and *CHX14*::GUS) or in soil by spraying a 0.05% phosphinothricine (BASTA) on 1-week-old seedlings (for *CHX08*::GUS and *CHX23*::GUS). Ten independent T1 lines for each construct were obtained and at least five independent homozygous T2 lines for each construct were examined for GUS expression.

Histochemical Staining of GUS Activity

Histochemical assays for GUS activity in T2 generation of *Arabidopsis* transgenic plants were performed according to the protocol described previously (Lagarde et al., 1996; Cheng et al., 2003). Three-week-old seedlings and fresh tissues such as leaves, roots, stems, and flowers from 6- to 8-week mature flowering transgenic plants were rinsed three times with staining buffer lacking 5-bromo-4-chloro-3-indolyl β -D-glucuronide (X-gluc; 50 mM sodium phosphate, pH 7.2, 0.5 mM $\text{K}_2\text{Fe}[\text{CN}]_6$, 0.5 mM $\text{K}_3\text{Fe}[\text{CN}]_6$), and then incubated for 16 h at 37°C in staining buffer containing 1 mM X-gluc. To clear chlorophyll from the green tissues, the stained seedlings were incubated in 70% ethanol overnight at 4°C and then kept in 95% ethanol. Cross-sections of GUS-stained material were prepared with a microtome (LKB, Bromma, Sweden) from tissues embedded in hydroxyethyl methacrylate (Technovit 7100; Heraeus-Kulzer, Wehrein, Germany) and counterstained in purple with periodic acid Schiff reagents. GUS staining patterns were recorded using a Zeiss Axiophot microscope (Zeiss, Jena, Germany) or a Nikon Eclipse E600 microscope (Nikon Instruments, Melville, NY) equipped with a differential interference contrast lens. Images were processed using Adobe Photoshop software (version 6.0; Adobe Systems, San Jose, CA).

Genome Array Analyses of Pollen

Spore Isolation

For spore isolation, *Arabidopsis* ecotype *Ler* plants were grown in controlled-environment cabinets at 21°C under illumination of $150 \mu\text{mol m}^{-2} \text{s}^{-1}$ with a 16-h photoperiod. Mature pollen was isolated according to Honys and Twell (2003). Isolated spores from three stages of immature male gametophytes were obtained by modification of the protocol of Kyo and Harada (1985, 1986). After removal of open flowers, inflorescences (bud clusters) from 400 plants were collected and gently ground using a mortar and pestle in 0.3 M mannitol. The slurry was filtered through 100 and 53 μm nylon mesh. Mixed spores were concentrated by centrifugation (50-mL Falcon tubes, 450g, 3 min, 4°C). Concentrated spores were loaded onto the top of 25%:45%:80% Percoll step gradient in a 10-mL centrifuge tube and centrifuged (450g, 5 min, 4°C). Three fractions were obtained containing microspores mixed with tetrads; microspores mixed with bicellular pollen; and tricellular pollen. Fraction 2 was diluted with 1 volume of 0.3 M mannitol loaded onto the top of a 25%:30%:45% Percoll step gradient and centrifuged again under the same conditions. Three subfractions of immature pollen were obtained: microspores; microspores and bicellular pollen mixture; and bicellular pollen. Spores in each fraction were concentrated by centrifugation (Eppendorf tubes, 2,000g, 1 min, 4°C) and stored at -80°C . The purity of isolated fractions was determined by light microscopy and 4',6-diamino-phenylindole staining, according to Park et al. (1998). Vital staining of isolated spore populations was assessed by fluorescein 3',6'-diacetate treatment (Eady et al., 1995).

DNA Chip Hybridization

Total RNA was extracted from 50 mg of isolated spores at each developmental stage using the RNeasy plant kit (Qiagen, Valencia, CA) according to the manufacturer's instructions. The yield and RNA purity were determined spectrophotometrically and using an Agilent 2100 Bioanalyzer (Agilent Technologies, Boblingen, Germany) at the Nottingham Arabidopsis Stock Centre.

Biotinylated target RNA was prepared from 20 μg of total RNA as described in the Affymetrix GeneChip Expression Analysis Technical Manual

(Affymetrix, Santa Clara, CA). Double-stranded cDNA was synthesized using SuperScript Choice System (Life Technologies/Gibco-BRL, Cleveland) with oligo(dT)₂₄ primer fused to T7 RNA polymerase promoter. Biotin-labeled target cRNA was prepared by cDNA in vitro transcription using the BioArray High-Yield RNA transcript labeling kit (Enzo Biochem, Farmingdale, NY) in the presence of biotinylated UTP and CTP.

Arabidopsis ATH1 genome arrays containing more than 24,000 genes were hybridized with 15 µg of labeled target cRNA for 16 h at 45°C. Microarrays were stained with Streptavidin-Phycoerythrin solution and scanned with an Agilent 2500A GeneArray Scanner (Agilent Technologies).

Data Analysis

Affymetrix Microarray Analysis Suite 5.0 standard image analysis was performed (Affymetrix). Sporophytic data from public baseline GeneChip experiments used for comparison with the pollen transcriptome were downloaded from the GARNet Web site (<http://www.arabidopsis.info>). In order to make data from all samples comparable, hybridization signals were scaled such that the top 2% and bottom 2% of signal intensities were excluded and the trimmed mean calculated as described by Welle et al. (2002). All signal values were multiplied by a microarray-specific scaling factor such that the 2% trimmed mean was normalized to 100. Scaling factors of the 46 microarrays used (Supplemental Table I) ranged from 0.293 to 1.649, with most (40) falling within the 3.5-fold range. In cases where more than one dataset for a particular tissue was available, the expression signal represents a mean value of all normalized experiments. To eliminate false positives, expressed genes were selected if they showed reliable expression values in all replicates. Genes with borderline expression were omitted.

Dataset codes downloaded from the GARNet Web site were as follows. COT: cotyledon stage 1.0 (Cornah [COT1-3], Villadsen [COT2-1], Short [COT3-1], Rente [COT4-1], Greville [COT5-3]– Cornah_A4-cornah-wsx_SLD_REP1-3, Villadsen_A1-villa-zer_SLD, Short_A2-mcain-con, A3-Rente-WS2-Control_SLD, Greville_A-01-grevi-CC1-3_SLD); SPR: sporophyte at stage 3.9 (Shirras– Shirr-Col-REP1-4); LEF: leaves (Heggie [LEF1-2], Lloyd [LEF2-3], Greco [LEF3-1]– A5-HEGGI-CAW, A4-LLOYD-CON_REP1-3, A2-Greco-WT); PET: petioles (Millenaar– Millenaar_A1-MILL-AIR-REP1-3); STT: stem top part (Turner– Turner_A5-Turne-WT-Top1-2_SLD); STB: stem base (Turner– Turner_A7-Turne-WT-Base1-2_SLD); ROT: roots (Yap [ROT1-1], Urwin [ROT2-1], Filleur [ROT3-2]– Yap_A2-AMF, Urwin_A-1-Urwin-Con_SLD, Sophie_A1-fille-WTw_SLD); RHR: root hair zone (Jones– Jones_A1-jones-WT1-2_SLD); SUS: cell suspension culture (Willats [SUS1-3], Swidzinski [SUS2-3]– A1-WILLA-CON-REP1-3, Swidzinski Control AGA Replicate 1-3). The number after the dash indicates the number of replicates used in each experiment.

RT-PCR Analysis

Total RNA was isolated from root, leaf, or pollen of *Arabidopsis* (Col-0) plants by the guanidine/acid-phenol method (Chomczynski and Sacchi, 1987). Briefly, root tissues were dissected from seedlings grown on one-half strength Murashige and Skoog medium for 7 d under 16-h-light/8-h-dark cycles. Rosette leaves (1 g fresh weight) were harvested from 3-week-old plants grown in soil under 16-h-light/8-h-dark conditions. Pollen grains were collected from the inflorescence of 5- to 6-week-old plants (Hony and Twell, 2003), and about 0.1 mg of RNA was isolated from 0.2 mL of pollen. RNA samples were treated with DNase to minimize any contamination of genomic DNA. One microgram of total RNA isolated from roots, leaves, or pollen were reverse transcribed in a 20-µL reaction using SuperScript II reverse transcriptase (Invitrogen, Carlsbad, CA). To ensure that the quantity of cDNA template was equivalent, 3 µL of first-strand cDNA were used in a reaction mixture for 30 PCR reactions. Gene-specific primers (Supplemental Table II) were then added to individual aliquots. About one-half of the primer sets spanned an intron. The condition used to amplify *CHX* genes was 94°C for 2 min followed by 35 cycles of 94°C (30 s), 55°C (30 s), and 72°C (90 s). Actin 11 (At3g12110) or *VHA-c1* (At4g34720) was amplified to verify equivalent loading of cDNA from different tissues. The forward (*c1-F* 5'-GATTTAAGATCTCAGATACAAA-ACTCCGAC-3') and reverse *VHA-c1* (*c1-R* 5'-TCCTACAATAAGCC-CGTAAAGAGCAAGCGC-3') primers corresponded to the 5'-untranslated region and a part of the coding region, respectively. Sense and antisense primers for actin 11 (At3g12110) were 5'-ATGGCAGATGGTGAAGACAT-TCAG-3' and 5'-GAAGCACTTCTGTGGACTATTGA-3', respectively. The fidelity of *CHX* amplified from pollen cDNA was confirmed by directly sequencing the PCR fragments (Maunula et al., 1999).

Bioinformatic Analyses

Revising *AtCHX* Protein Sequences

Alignment of predicted *CHX* proteins (e.g. <http://mips.gsf.de>) initially by ClustalW (Thompson et al., 1994) revealed potential errors in nearly one-half the protein sequences. A few full-length cDNAs available were translated and used to identify intron/exon borders in genomic sequences. These *CHX* proteins were used as guides to predict coding sequences of the closest relatives by translating the genomic sequences. Other sequences were verified after full-length cDNA was amplified from the pollen message and sequenced. The revised gene models will be deposited in GenBank (<http://www.ncbi.nlm.nih.gov>) and PlantsT (<http://plantst.sdsc.edu>) databases.

Finding Rice *CHX* Genes

Selected *AtCHX* and a few *OsCHX* proteins collected from the Rice Membrane Protein Library (<http://www.cbs.umn.edu/rice>) were used to conduct TBLASTN (Altschul et al., 1997) against the Rice Annotated Protein Database at TIGR (including all sequences predicted from the International Rice Genome Sequencing Project). This search produced significant alignments with proteins from BAC/PAC clones, as well as full-length cDNAs (<http://cdna01.dna.affrc.go.jp/cDNA>) from the *japonica* subspecies of rice (*Oryza sativa*; Kikuchi et al., 2003). Sequences were then verified with those from TIGR (<http://www.tigr.org/tdb/e2k1/osa1/index.shtml>) and later from Aramemnon (<http://aramemnon.botanik.uni-koeln.de>). To confirm the cDNA sequence, BLASTN between cDNA and genomic sequences was performed. Protein sequences predicted from genomic DNA were compared with that translated from cDNA. In a few cases, an error due to a missing base in the cDNA was corrected to give the predicted protein.

Phylogenetic Analyses

Proteins were compared by multiple alignments using the T-Coffee program (Notredame et al., 2000; <http://igs-server.cnrs-mrs.fr/Tcoffee>). Bootstrap analyses for each branch were performed 1,000 times using PAUP 4.0b10 9 (Swofford, 1998). Specific details are described in the figure legends. Other programs used were Treeview for graphic output.

Upon request, all novel materials described in this publication will be made available in a timely manner for noncommercial research purposes, subject to the requisite permission from any third-party owners of all or parts of the material. Obtaining any permission will be the responsibility of the requestor.

Note Added in Proof

In contrast to our finding of *CHX23* (At1g05580) expression in pollen using three independent methods, a recent paper by Song et al. (Song CP, Guo Y, Qiu Q, Lambert G, Galbraith DW, Jagendorf A, Zhu JK [2004] A probable Na⁺(K⁺)/H⁺ exchanger on the chloroplast envelope functions in pH homeostasis and chloroplast development in *Arabidopsis thaliana*. *Proc Natl Acad Sci USA* 101: 10211–10216) showed that *AtCHX23* is predominantly expressed in vegetative tissues. The reason for this discrepancy is unclear. The study by Song et al. is not sufficiently documented to verify the specific promoter region used for GUS expression or the specificity of the RT-PCR product.

ACKNOWLEDGMENTS

Transgenic plants expressing *AtCHX13::GUS* (from F.C.) were generated as part of the GENOPLANTE program AF 1999–062 (Functional analysis of *Arabidopsis* genes involved in mineral nutrition and response to abiotic stress). Preliminary analyses of *AtCHX* genes and their promoters were conducted by Eric P. Nawrocki (University of Maryland, College Park, MD). H.S. gratefully acknowledges stimulating discussions with Charles Delwiche (University of Maryland, College Park, MD). D.T. gratefully acknowledges support from the Biotechnology and Biological Sciences Research Council and the GARNet transcriptome center at Nottingham *Arabidopsis* Stock Centre for performing pollen microarray hybridizations.

Received May 14, 2004; returned for revision June 14, 2004; accepted July 12, 2004.

LITERATURE CITED

- Ali R, Brett CL, Mukherjee S, Rao R (2004) Inhibition of sodium/proton exchange by a Rab-GTPase-activating protein regulates endosomal traffic in yeast. *J Biol Chem* **279**: 4498–4506
- Altschul SF, Madden TL, Schäffer AA, Zhang J, Zhang Z, Miller W, Lipman DJ (1997) Gapped BLAST and PSI-BLAST: a new generation of protein database search programs. *Nucleic Acids Res* **25**: 3389–3402
- Apse MP, Aharon GS, Snedden WA, Blumwald E (1999) Salt tolerance conferred by overexpression of a vacuolar Na⁺/H⁺ antiport in *Arabidopsis*. *Science* **285**: 1256–1258
- Arabidopsis Genome Initiative (2000) Analysis of the genome sequence of the flowering plant *Arabidopsis thaliana*. *Nature* **408**: 796–815
- Becker JD, Boavida LC, Carneiro J, Haury M, Feijo JA (2003) Transcriptional profiling of *Arabidopsis* tissues reveals the unique characteristics of the pollen transcriptome. *Plant Physiol* **133**: 713–725
- Birnbaum K, Shasha DE, Wang JY, Jung JW, Lambert GM, Galbraith DW, Benfey PN (2003) A gene expression map of the *Arabidopsis* root. *Science* **302**: 1956–1960
- Booth IR, Jones MA, McLaggan D, Nikolaev Y, Ness LS, Wood CM, Miller S, Totemeyer S, Ferguson GP (1996) Bacterial ion channels. In: WN Konings, HR Kaback, JS Jolkema, eds, *Handbook of Biological Physics*, Vol 2. Elsevier Science, Amsterdam, pp 693–729
- Bowers K, Levi BP, Patel FI, Stevens TH (2000) The sodium/proton exchanger Nhx1p is required for endosomal protein trafficking in the yeast *Saccharomyces cerevisiae*. *Mol Biol Cell* **11**: 4277–4294
- Boyes DC, Zayed AM, Ascenzi R, McCaskill AJ, Hoffman NE, Davis KR, Gortlach J (2001) Growth stage-based phenotypic analysis of *Arabidopsis*: a model for high throughput functional genomics in plants. *Plant Cell* **13**: 1499–1510
- Brett CL, Wei Y, Donowitz M, Rao R (2002) Human Na⁺/H⁺ exchanger isoform 6 is found in recycling endosomes of cells, not in mitochondria. *Am J Physiol Cell Physiol* **282**: 1031–1041
- Cellier F, Conejero G, Ricaud L, Luu DT, Lepetit M, Gosti F, Casse F (2004) Characterization of AtCHX17, a member of the cation/H⁺ exchanger CHX family, from *A. thaliana* suggests a role in K⁺ homeostasis. *Plant J* (in press)
- Cheng N-H, Pittman JK, Barkla BJ, Shigaki T, Hirschi KD (2003) The *Arabidopsis* cax1 mutant exhibits impaired ion homeostasis, development, and hormonal responses and reveals interplay among vacuolar transporters. *Plant Cell* **15**: 347–364
- Chomczynski P, Sacchi N (1987) Single-step method of RNA isolation by acid guanidinium thiocyanate-phenol-chloroform extraction. *Anal Biochem* **162**: 156–159
- Clough SJ, Bent AF (1998) Floral dip: a simplified method for *Agrobacterium*-mediated transformation of *Arabidopsis thaliana*. *Plant J* **16**: 735–743
- Eady C, Twell D, Lindsey K (1995) Pollen viability and transgene expression following storage in honey. *Transgenic Res* **4**: 226–231
- Eshed Y, Baum SE, Perea JV, Bowman JL (2001) Establishment of polarity in lateral organs of *Arabidopsis*. *Curr Biol* **11**: 1251–1260
- Feijo JA, Sainhas J, Hackett GR, Kunkel JG, Hepler PK (1999) Growing pollen tubes possess a constitutive alkaline band in the clear zone and a growth-dependent acidic tip. *J Cell Biol* **144**: 483–496
- Feijo JA, Sainhas J, Holdaway-Clarke T, Cordeiro MS, Kunkel JG, Hepler PK (2001) Cellular oscillations and the regulation of growth: the pollen tube paradigm. *Bioessays* **23**: 86–94 (Review)
- Ferguson GP, Nikolaev Y, McLaggan D, Maclean M, Booth IR (1997) Survival during exposure to the electrophilic reagent N-ethylmaleimide in *Escherichia coli*: role of KefB and KefC potassium channels. *J Bacteriol* **179**: 1007–1012
- Gaxiola RA, Rao R, Sherman A, Grisafi P, Alper SL, Fink GR (1999) The *Arabidopsis thaliana* proton transporters, AtNhx1 and Avp1, can function in cation detoxification in yeast. *Proc Natl Acad Sci USA* **96**: 1480–1485
- Gleaves AP (1992) A versatile binary vector system with a T-DNA organizational structure conducive to efficient integration of cloned DNA into the plant genome. *Plant Mol Biol* **20**: 1203–1207
- Hepler PK, Vidali L, Cheung AY (2001) Polarized cell growth in higher plants. *Annu Rev Cell Dev Biol* **17**: 159–187
- Hoagland DR (1944) Lectures on the Inorganic Nutrition of Plants. *Chronica Botanica*, Waltham, MA
- Holdaway-Clarke TL, Hepler PK (2003) Control of pollen tube growth: role of ion gradients and fluxes. *New Phytol* **159**: 539–563
- Honys D, Twell D (2003) Comparative analysis of the *Arabidopsis* pollen transcriptome. *Plant Physiol* **132**: 640–652
- Inaba M, Sakamoto A, Murata N (2001) Functional expression in *Escherichia coli* of low-affinity and high-affinity Na⁺, Li⁺/H⁺ antiporters of *Synechocystis*. *J Bacteriol* **183**: 1376–1384
- Kikuchi S, Satoh K, Nagata T, Kawagashira N, Doi K, Kishimoto N, Yazaki J, Ishikawa M, Yamada H, Ooka H, et al (2003) Collection, mapping, and annotation of over 28,000 cDNA clones from japonica rice. *Science* **301**: 376–379
- Kinclova O, Ramos J, Potier S, Sychrova H (2001) Functional study of the *Saccharomyces cerevisiae* Nha1p C-terminus. *Mol Microbiol* **40**: 656–668
- Koncz C, Shell J (1986) The promoter of TL-DNA gene 5 controls the tissue specific expression of chimaeric genes carried by a novel type of *Agrobacterium* binary vector. *Mol Gen Genet* **204**: 383–396
- Kreps JA, Wu Y, Chang HS, Zhu T, Wang X, Harper JF (2002) Transcriptome changes for *Arabidopsis* in response to salt, osmotic, and cold stress. *Plant Physiol* **130**: 2129–2141
- Kyo M, Harada H (1985) Studies on conditions for cell division and embryogenesis in isolated pollen culture of *Nicotiana rustica*. *Plant Physiol* **79**: 90–94
- Kyo M, Harada H (1986) Control of the developmental pathway of tobacco pollen in vitro. *Planta* **168**: 427–432
- Lagarde D, Basset M, Lepetit M, Conéjéro G, Gaymard F, Astruc S, Grignon C (1996) Tissue-specific expression of *Arabidopsis* AKT1 gene is consistent with a role in K⁺ nutrition. *Plant J* **9**: 195–203
- Martin WH, Beavis AD, Garlid KD (1984) Identification of an 82,000-dalton protein responsible for K⁺/H⁺ antiport in rat liver mitochondria. *J Biol Chem* **259**: 2062–2065
- Maser P, Thomine S, Schroeder JI, Ward JM, Hirschi K, Sze H, Talke IN, Antmann A, Maathius FL, Sanders D, et al (2001) Phylogenetic relationships within cation-transporter families of *Arabidopsis thaliana*. *Plant Physiol* **126**: 1646–1667
- Maunula L, Piiparinen H, von Bonsdorff CH (1999) Confirmation of Norwalk-like virus amplicons after RT-PCR by microplate hybridization and direct sequencing. *J Virol Methods* **83**: 125–134
- Messerli MA, Danuser G, Robinson KR (1999) Pulsatile influxes of H⁺, K⁺ and Ca²⁺ lag growth pulses of *Lilium longiflorum* pollen tubes. *J Cell Sci* **112**: 1497–1509
- Miller S, Douglas RM, Carter P, Booth IR (1997) Mutations in the glutathione-gated KefC K⁺ efflux system of *Escherichia coli* that cause constitutive activation. *J Biol Chem* **272**: 24942–24947
- Mouline K, Very AA, Gaymard F, Boucherez J, Pilot G, Devic M, Bouchez D, Thibaud JB, Sentenac H (2002) Pollen tube development and competitive ability are impaired by disruption of a Shaker K⁺ channel in *Arabidopsis*. *Genes Dev* **16**: 339–350
- Nass R, Rao R (1998) Novel localization of a Na⁺/H⁺ exchanger in a late endosomal compartment of yeast: implications for vacuole biogenesis. *J Biol Chem* **273**: 21054–21060
- Notredame C, Higgins DG, Heringa J (2000) T-Coffee: a novel method for fast and accurate multiple sequence alignment. *J Mol Biol* **302**: 205–217
- Numata M, Orłowski J (2001) Molecular cloning and characterization of a novel (Na⁺,K⁺)/H⁺ exchanger localized to the trans-Golgi network. *J Biol Chem* **276**: 17387–17394
- Orłowski J, Kandasamy RA, Shull GE (1992) Molecular cloning of putative members of the Na/H exchanger gene family. cDNA cloning, deduced amino acid sequence, and mRNA tissue expression of the rat Na/H exchanger NHE-1 and two structurally related proteins. *J Biol Chem* **267**: 9331–9339
- Park SK, Howden R, Twell DP (1998) The *Arabidopsis thaliana* gametophytic mutation pollen1 disrupts microspore polarity, division asymmetry and pollen cell fate. *Development* **125**: 3789–3799
- Putney LK, Denker SP, Barber DL (2002) The changing face of the Na⁺/H⁺ exchanger, NHE1: structure, regulation, and cellular actions. *Annu Rev Pharmacol Toxicol* **42**: 527–552
- Qiu QS, Guo Y, Dietrich MA, Schumaker KS, Zhu J-K (2002) Regulation of SOS1, a plasma membrane Na⁺/H⁺ exchanger in *Arabidopsis thaliana*, by SOS2 and SOS3. *Proc Natl Acad Sci USA* **99**: 8436–8441
- Ramirez J, Ramirez O, Saldana C, Coria R, Pena A (1998) A *Saccharomyces cerevisiae* mutant lacking a K⁺/H⁺ exchanger. *J Bacteriol* **180**: 5860–5865
- Roosild TP, Miller S, Booth IR, Choe S (2002) A mechanism of regulating

- transmembrane potassium flux through a ligand-mediated conformational switch. *Cell* **109**: 781–791
- Saier MH Jr** (2000) A functional-phylogenetic classification system for transmembrane solute transporters. *Microbiol Mol Biol Rev* **64**: 354–411
- Sambrook JF, Fritsch EF, Maniatis T** (1989) *Molecular Cloning: A Laboratory Manual*, Ed 2. Cold Spring Harbor Laboratory Press, Cold Spring Harbor, NY
- Scholz-Starke J, Buttner M, Sauer N** (2003) AtSTP6, a new pollen-specific H⁺-monosaccharide symporter from Arabidopsis. *Plant Physiol* **131**: 70–77
- Schwacke R, Grallath S, Breitreuz KE, Stransky E, Stransky H, Frommer WB, Rentsch D** (1999) LeProT1, a transporter for proline, glycine betaine, and gamma-amino butyric acid in tomato pollen. *Plant Cell* **11**: 377–392
- Shi H, Ishitani M, Kim C, Zhu JK** (2000) The Arabidopsis thaliana salt tolerance gene SOS1 encodes a putative Na⁺/H⁺ antiporter. *Proc Natl Acad Sci USA* **97**: 6896–6901
- Shi H, Lee BH, Wu SJ, Zhu JK** (2003) Overexpression of a plasma membrane Na⁺/H⁺ antiporter gene improves salt tolerance in *Arabidopsis thaliana*. *Nat Biotechnol* **21**: 81–85
- Shi H, Quintero FJ, Pardo JM, Zhu JK** (2002) The putative plasma membrane Na⁺/H⁺ antiporter SOS1 controls long-distance Na⁺ transport in plants. *Plant Cell* **14**: 465–477
- Southworth TW, Guffanti AA, Moir A, Krulwich TA** (2001) GerN, an endospore germination protein of *Bacillus cereus*, is an Na⁺/H⁺-K⁺ antiporter. *J Bacteriol* **183**: 5896–5903
- Swofford DL** (1998) PAUP*. *Phylogenetic Analysis Using Parsimony (*and Other Methods)*. Version 4. Sinauer Associates, Sunderland, MA
- Thompson JD, Higgins DG, Gibson TJ** (1994) CLUSTAL W: improving the sensitivity of progressive multiple sequence alignment through sequence weighting, position specific gap penalties and weight matrix choice. *Nucleic Acids Res* **22**: 4673–4680
- Twiss D** (2002) Pollen developmental biology. In SD O'Neill, JA Roberts, eds, *Plant Reproduction. Annual Plant Reviews*, Vol 6. Sheffield Academic Press, Sheffield, UK, pp 86–153
- Venema K, Belver A, Marin-Manzano MC, Rodriguez-Rosales MP, Donaire JP** (2003) A novel intracellular K⁺/H⁺ antiporter related to Na⁺/H⁺ antiporters is important for K⁺ ion homeostasis in plants. *J Biol Chem* **278**: 22453–22459
- Venema K, Quintero FJ, Pardo JM, Donaire JP** (2002) The Arabidopsis Na⁺/H⁺ exchanger AtNHX1 catalyzes low affinity Na⁺ and K⁺ transport in reconstituted liposomes. *J Biol Chem* **277**: 2413–2418
- Walker DJ, Leigh RA, Miller AJ** (1996) Potassium homeostasis in vacuolate plant cells. *Proc Natl Acad Sci USA* **93**: 10510–10514
- Waser M, Hess-Bienz D, Davies K, Solioz M** (1992) Cloning and disruption of a putative NaH-antiporter gene of *Enterococcus hirae*. *J Biol Chem* **267**: 5396–5400
- Welle S, Brooks AI, Thornton CA** (2002) Computational method for reducing variance with Affymetrix microarrays. *BMC Bioinformatics* **3**: 23
- Wu W, Berkowitz GA** (1992) Stromal pH and photosynthesis are affected by electroneutral K⁺ and H⁺ exchange through chloroplast envelope ion channels. *Plant Physiol* **98**: 666–672
- Yamaguchi T, Fukada-Tanaka S, Inagaki Y, Saito N, Yonekura-Sakakibara K, Tanaka Y, Kusumi T, Iida S** (2001) Genes encoding the vacuolar Na⁺/H⁺ exchanger and flower coloration. *Plant Cell Physiol* **42**: 451–461
- Yokoi S, Quintero FJ, Cubero B, Ruiz MT, Bressan RA, Hasegawa PM, Pardo JM** (2002) Differential expression and function of Arabidopsis thaliana NHX Na⁺/H⁺ antiporters in the salt stress response. *Plant J* **30**: 529–539
- Yoshida Y, Nanjo T, Miura S, Yamaguchi-Shinozaki K, Shinozaki K** (1999) Stress-responsive and developmental regulation of Delta(1)-pyrroline-5-carboxylate synthetase 1 (P5CS1) gene expression in *Arabidopsis thaliana*. *Biochem Biophys Res Commun* **261**: 766–772